Supporting Information

3D dual network MOF-derived magnetic Co/Ni@C-GnP@PDMS composites for absorption-dominant EMI shielding with enhanced thermal conductivity

Tahreem Zahra[a], Muhammad Yasir[a,b], Sebastian Anand[c], Kayeon Kang[a], Sung-Ryong Kim[a,b]*

[a]*Department of Polymer Science and Engineering, Korea National University, Chungju 27469, Republic of Korea*

[b]*Department of IT - Energy Convergence (BK21 PLUS), Korea National University, Chungju 27469, Republic of Korea*

[c]*School of Chemistry and CRANN Institute, Trinity College Dublin, Dublin 2, Ireland*

***Corresponding author:** Sung-Ryong Kim, e-mail: srkim@ut.ac.kr

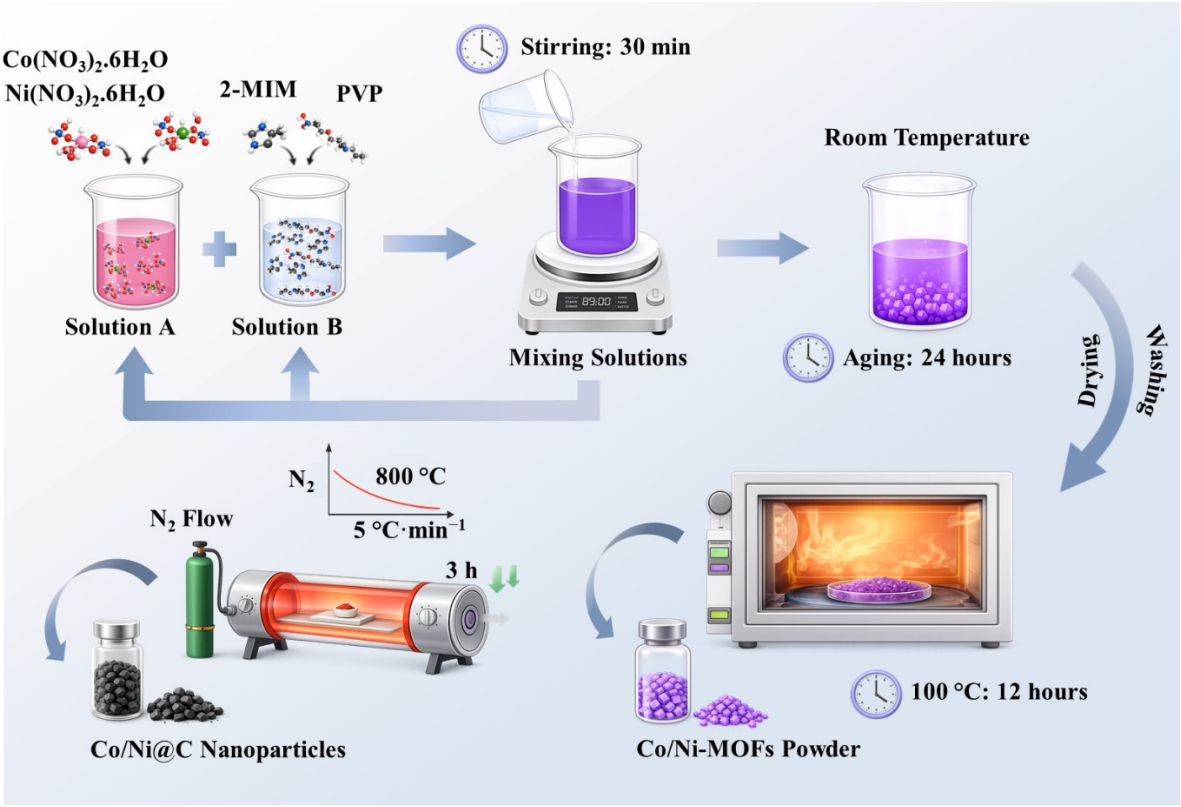

Fig. S1. Schematic representation of the preparation of Co/Ni-MOFs and Co/Ni@C carbonized magnetic nanoparticles.

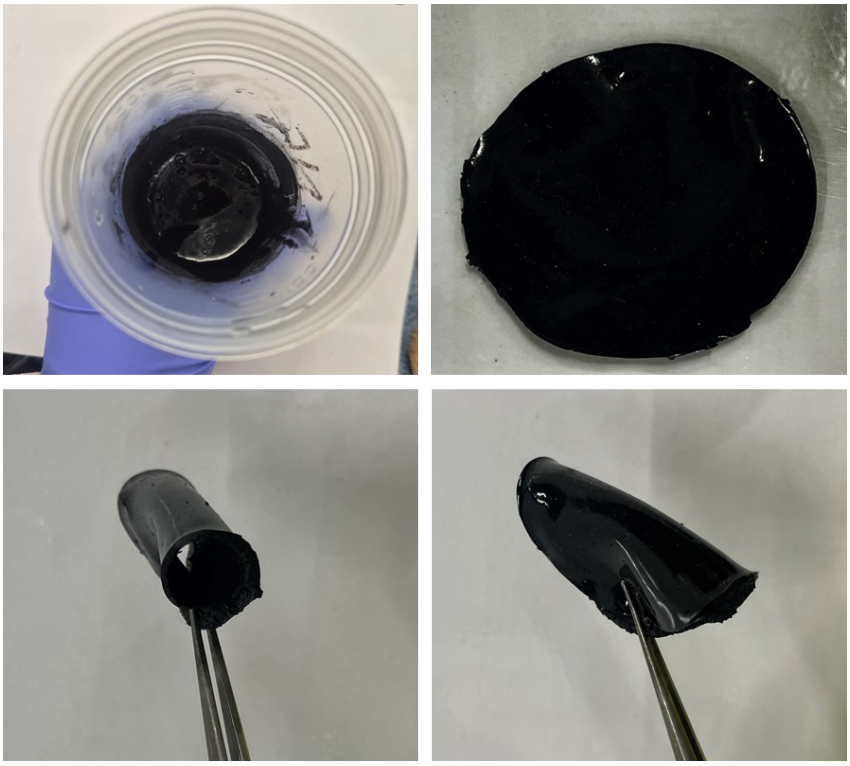

Fig. S2. Digital photographs of as-prepared Co/Ni@C@PDMS mixture and the corresponding cured Co/Ni@C@PDMS composite film.

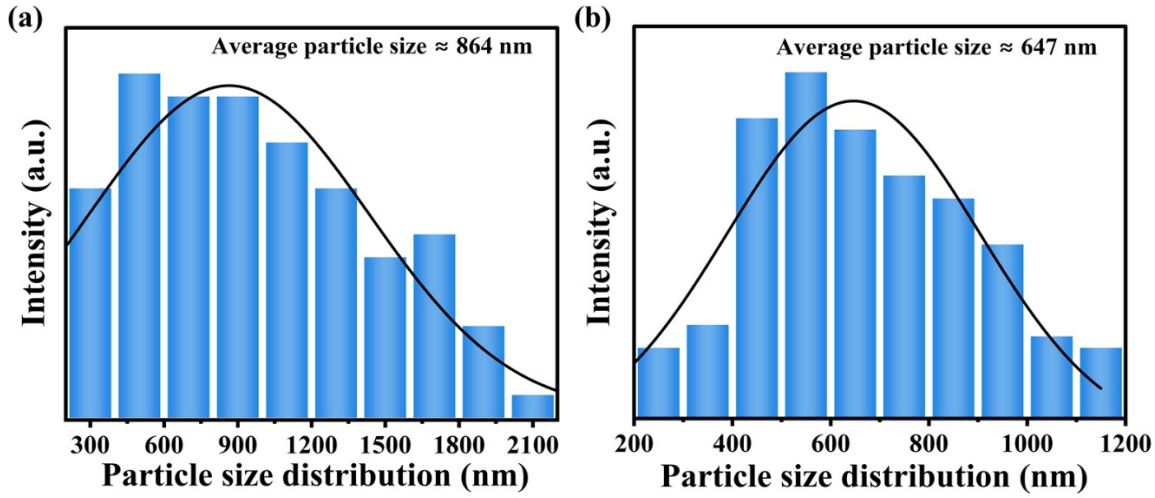

Fig. S3. Particle size distribution of (a) Pristine Co/Ni-MOFs before carbonization. (b) Co/Ni@C nanoparticles obtained after carbonization.

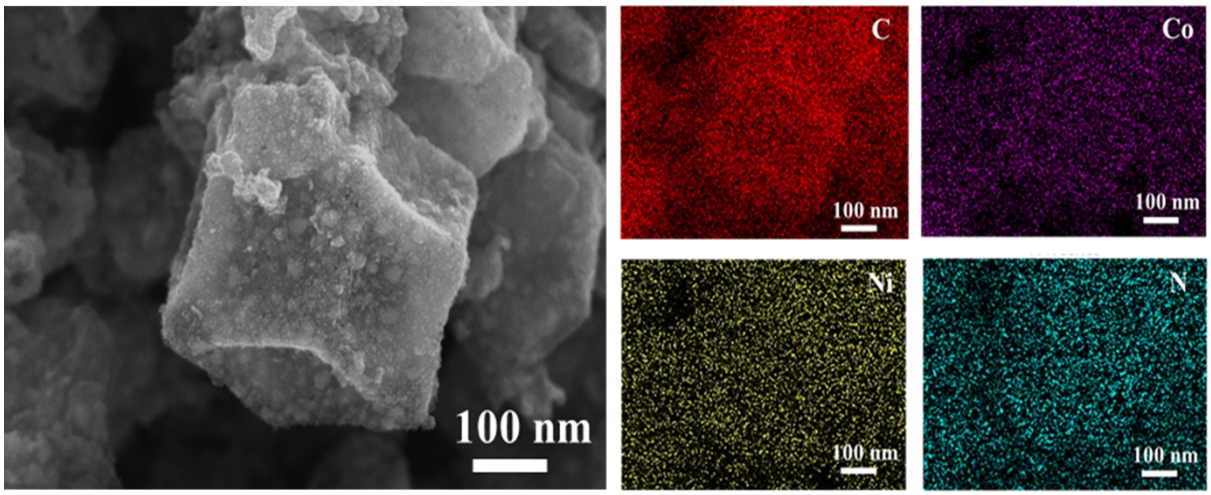

Fig. S4. EDS elemental mapping images showing the spatial distribution of C, Co, Ni and N elements in the Co/Ni@C nanoparticles.

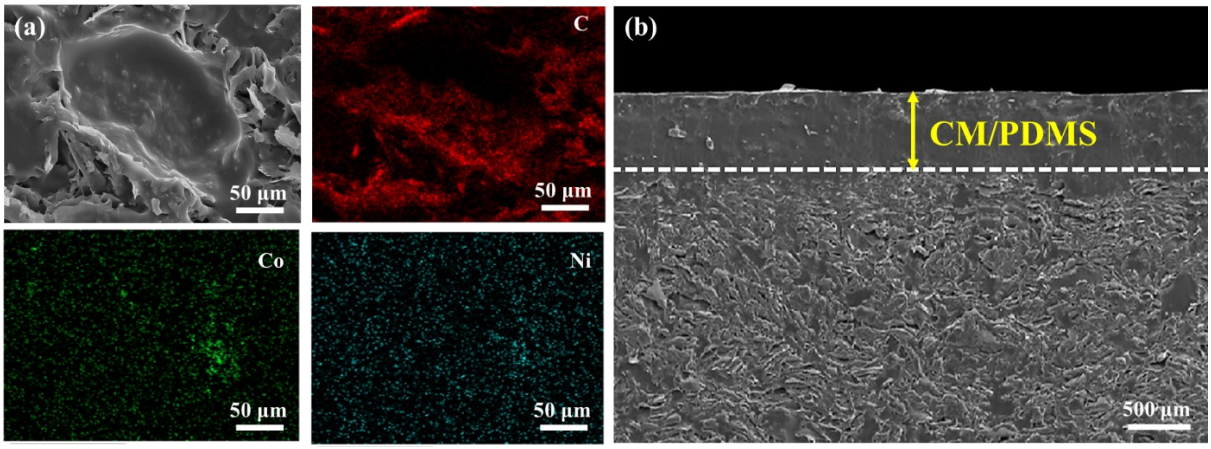

Fig. S5. (a) EDS elemental mapping images of C, Co, and Ni elements in the 3D dual GnP30@PDMS/CM5 composites. (b) Cross-sectional SEM image showing the CM/PDMS layer on the top side of the GnP30@PDMS/CM5 composites.

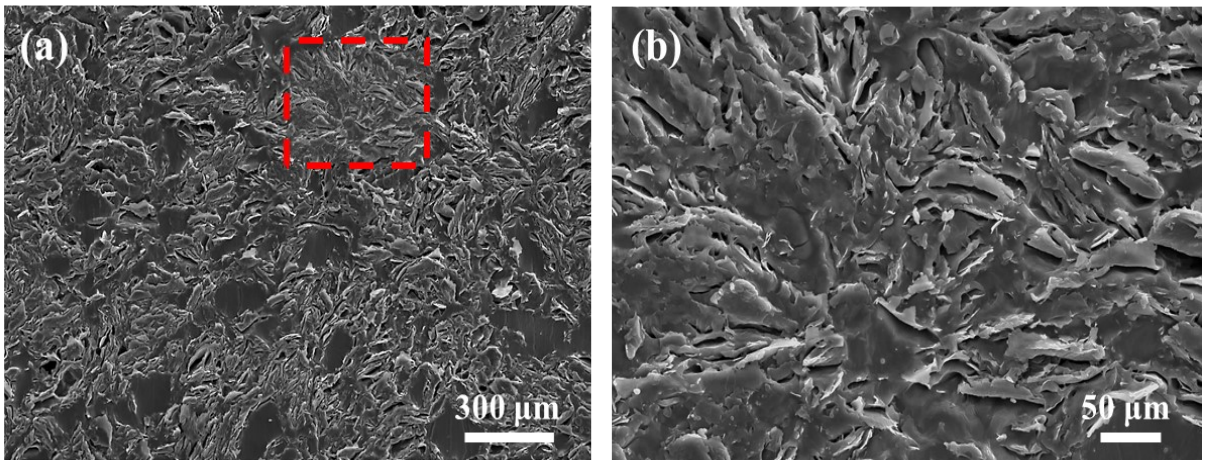

Fig. S6. Cross-sectional SEM images of random R-GnP30/CM5/PDMS composites at different magnifications.

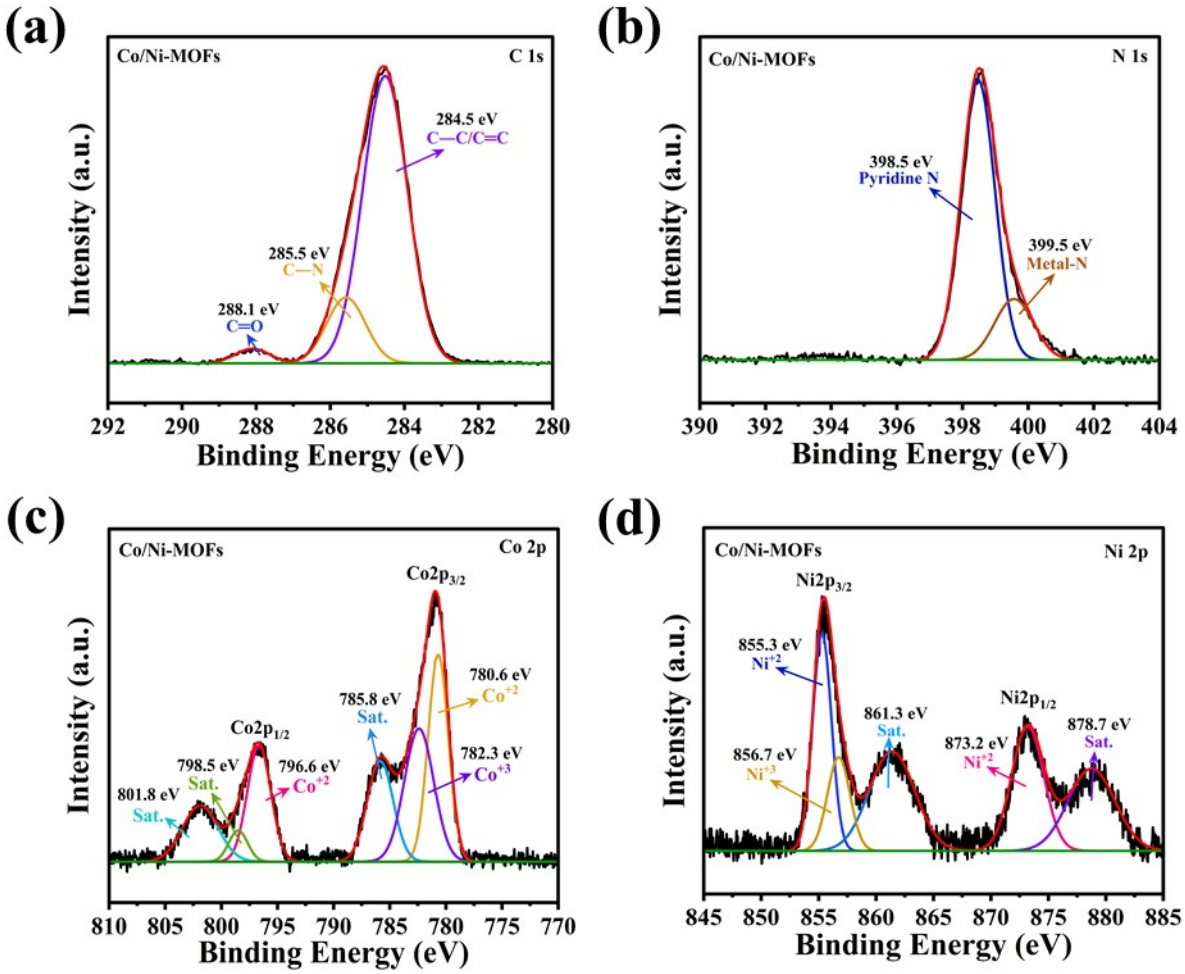

Fig. S7. High resolution XPS spectrum of (a) C 1s spectrum, (b) N 1s spectrum, (c) Co 2p spectrum, and (d) Ni 2p spectrum for Co/Ni-MOFs.

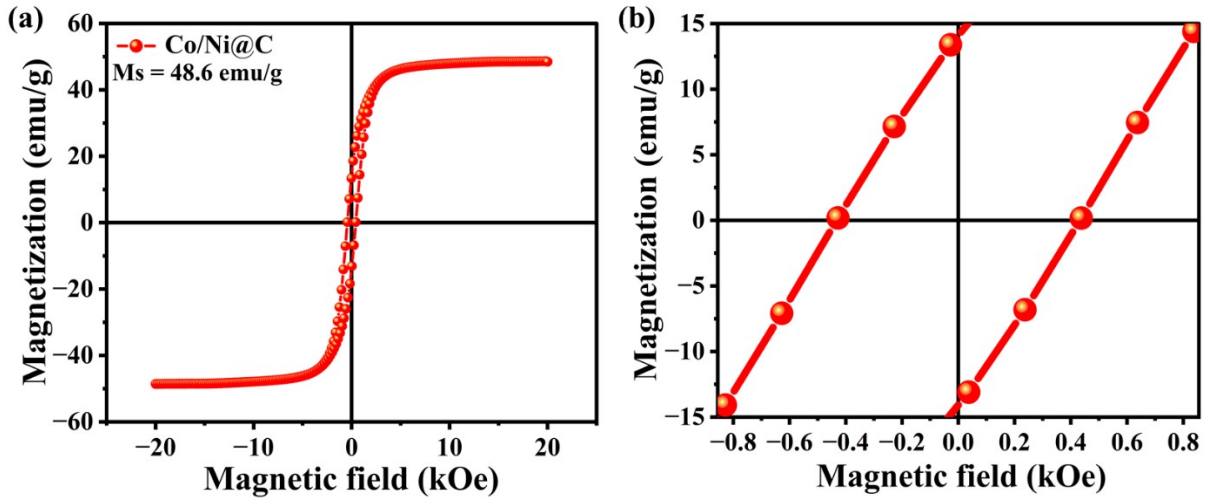

Fig. S8. (a-b) M-H hysteresis loops of carbonized Co/Ni@C nanoparticles.

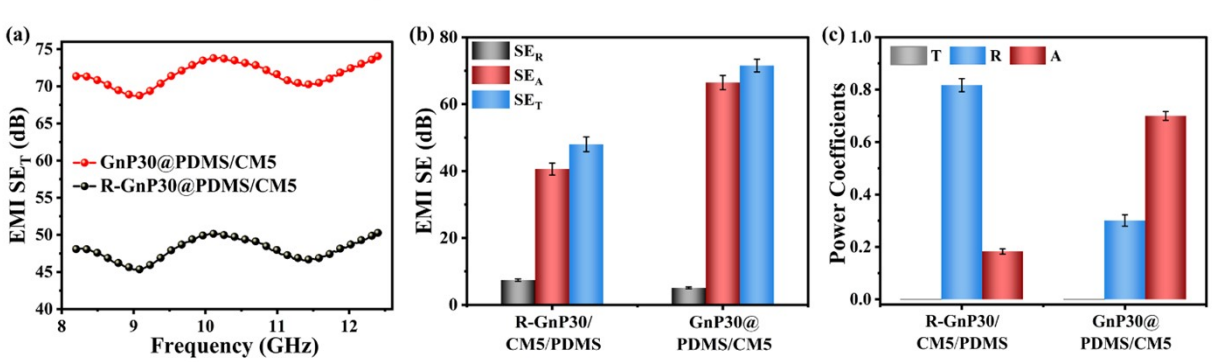

Fig. S9. Comparison of (a) EMI SE_T, (b) SE, and (c) corresponding power coefficients of

random R-GnP30/CM5/PDMS and 3D dual GnP30@PDMS/CM5 composites. Error bars represent standard deviation (n = 3).

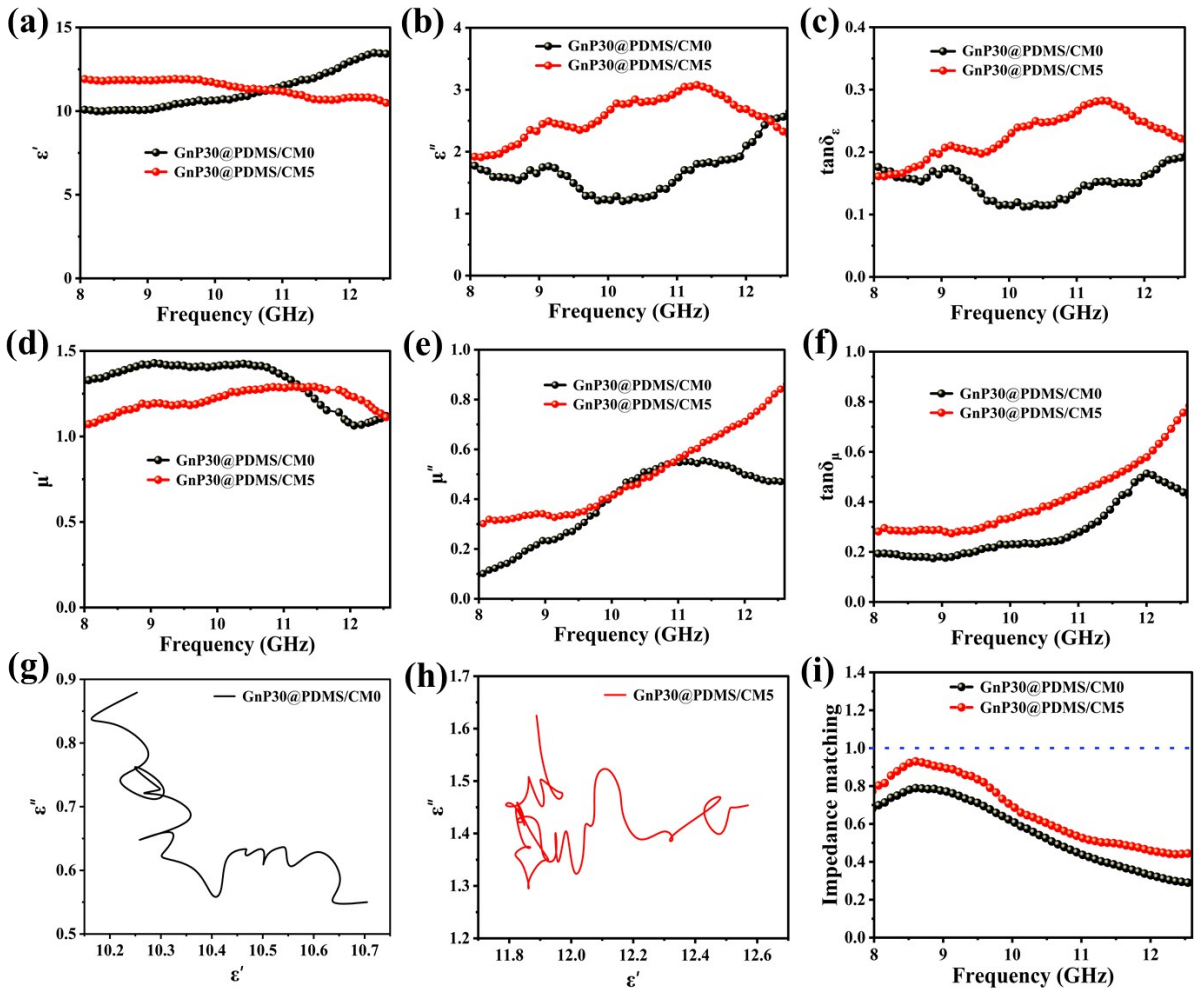

Fig. S10. Frequency-dependent electromagnetic parameters of GnP30@PDMS/CM composites. (a) ε', (b) ε'', and (c) tanδ_{ε}. (d) μ', (e) μ'', and (f) tanδ_{μ}. (g, h) Cole–Cole plots for GnP30@PDMS/CM0 and GnP30@PDMS/CM5, respectively. (i) Normalized input impedance ($|Z_{in}/Z_0|$) as a function of frequency.

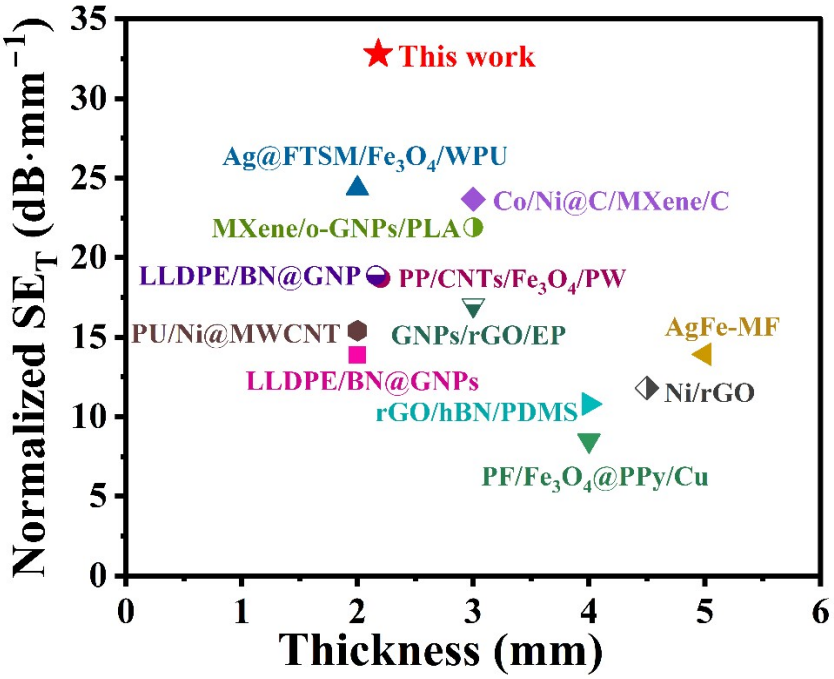

Fig. S11. Comparison of normalized SE_T versus thickness for the GnP30@PDMS/CM5 composite with 3D dual network structures and other reported 3D polymer composites.

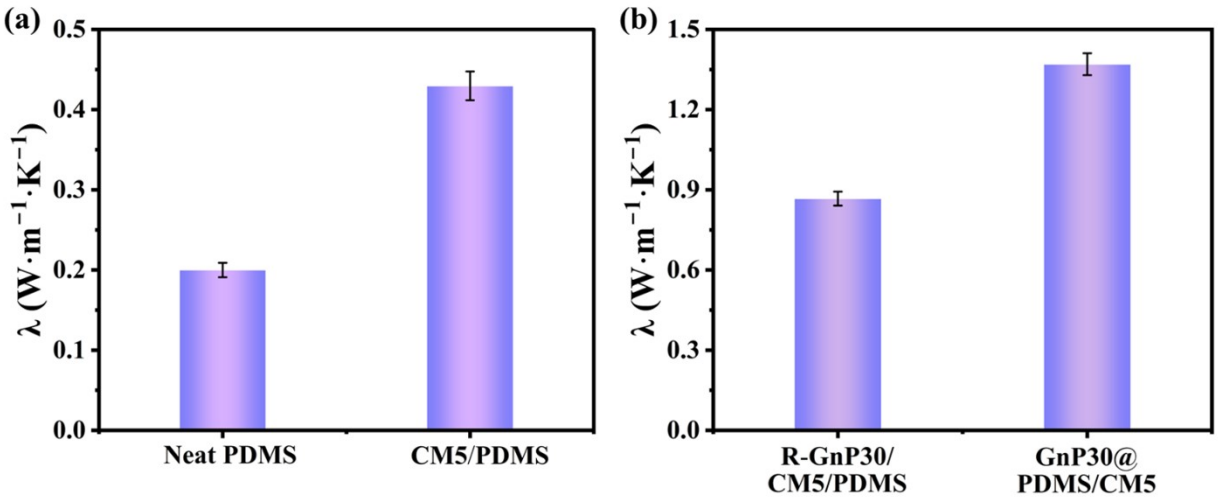

Fig. S12. Comparison of thermal conductivity of (a) neat PDMS and 5wt% CM/PDMS composites. (b) Random R-GnP30/CM5/PDMS composites and 3D dual GnP30@PDMS/CM5 composites. Error bars represent standard deviation (n = 3).

Table S1. Compositional analysis of GnP30@PDMS foams and GnP30@PDMS/CM composites with GnP and Co/Ni@C nanoparticles.

Materials	GnP content in GnP30@PDMS foams (wt%)	GnP content in GnP30@PDMS/CM composites (wt%)	Co/Ni@C content in GnP30@PDMS/CM composites (wt%)
GnP30@PDMS/CM0	30	15.85	-
GnP30@PDMS/CM3		15.97	2.25
GnP30@PDMS/CM5		16.06	3.70
GnP30@PDMS/CM8		16.25	5.98

Table S2. Detailed comparison of EMI shielding performance of our prepared 3D dual GnP30@PDMS/CM composites with other reported 3D dual structure-based composite materials.

Materials	Thickness (mm)	EMI SE (dB)	Normalized SE ($dB \cdot mm^{-1}$)	Absorption coefficient (A)	Year and references
LLDPE/BN@GNP	2	27.8	13.9	~0.48	2023[1]
PP/CNTs/Fe_3O_4/PW	2.2	39.2	17.8	~0.21	2022[2]
Ag@FTSM/Fe_3O_4/WPU	2	48.7	24.35	0.60	2024 [3]
PF/Fe_3O_4@PPy/Cu	4	32.2	8.05	0.60	2024[4]
Co/Ni@C/MXene/cellulose-derived carbon	3	70.4	23.67	0.54	2025[5]
PCL/BN@PLA/CNTs	3	31.4	10.5	~0.3	2024[6]
rGO/hBN/PDMS	4	43.1	10.8	0.34	2023[7]
PU/Ni@MWCNTs	2	30.8	15.40	-	2020[8]
GNPs/rGO/EP	3	51	17	~0.14	2019[9]
Graphene/CNT/PEN	2	25.8	16.1	-	2023[10]
rGF/rGM/PDMS	2.2	38.75	17.61	~0.47	2023[11]
MXene@rGO/PI	5	58.7	11.74	~0.19	2024[12]
PDMS/GNPs@LM	2.16	40.8	18.89	~0.3	2024[13]
MXene/o-GNPs/PLA	3	65	21.9	-	2022[14]
PVA/PAA@PEGDMA /PEDOT:PSS	4	40.61	10.15	0.36	2025[15]
GnP30@PDMS/CM5	2.18	71.5	32.8	0.69	**This work**

Abbreviation: LLDPE: Linear low-density polyethylene; BN: Boron nitride: Fe_3O_4: Iron oxide; PP: Polypropylene; FTSM: Foamed temperature-sensitive microspheres; CNT: Carbon nanotubes; PW: Paraffin wax; WPU: Waterborne polyurethane; PF: Polyimide foams; PPy: Polypyrrole; PCL: Polycaprolactone; rGO: Reduced graphene oxide; PDMS: PU: Polyurethane; MWCNTs: Multi-walled carbon nanotubes; PEN: Poly(aryl ether nitrile); rGF: rGO and Fe_3O_4; rGM: rGO and Fe_3O_4; LM: Liquid metal; o-GNPs: Ordered GNPs; PLA: Polylactic acid; PVA: Polyvinyl alcohol; PPA: Polyacrylic acid; PEGDMA: Polyethylene glycol dimethacrylate; PEDOT:PSS: Poly (3,4-ethylenedioxythiophene) polystyrene sulfonate).

Note: "~" indicates approximate values estimated from the corresponding figures in the cited references.

Table S3. Detailed comparison of through-plane thermal conductivity values in our prepared 3D dual GnP30@PDMS/CM5 composites with other reported 3D dual structure-based composite materials.

Materials	Filler content (wt%)	Thermal conductivity ($W \cdot m^{-1} \cdot K^{-1}$)	TCE (%)	Year and references
AlN/BN/EP	50	1.29	614	2021[16]
BN@CNTs/EP	30	1.20	500	2020[17]
PP/CNTs/Fe_3O_4/PW	10.6	0.59	211	2022[2]
CuNWs-TAGA/EP	7.2	0.71	132	2022[18]
EP/BN-PVDF	21	1.22	618	2020[19]
TiO_2@C-Ni/CNTs/NR	3	0.25	136	2022[20]
PP/CNTs/Fe_3O_4/PW	20	0.59	210	2022[2]
PDMS/Ag-BN/rGO	32	1.2	488	2021[21]
PU/GF/MAPP	40	0.58	82.8	2022[22]
rGO/hBN/PDMS	30	1.27	567	2023[7]
PVDF@MWCNT/BN	55	0.83	-	2019[23]
CMC@CNT-PPy/PW	19.1	0.64	156	2023[24]
C-MG-paraffin	15.1	0.88	300	2021[25]
GnP30@PDMS/CM5	19.76	1.37	585	**This work**

Abbreviation: AIN: Aluminum nitride; BN: Boron nitride: EP: Epoxy; CNT: Carbon nanotubes; PP: Polypropylene; Fe_3O_4: Iron oxide; PW: Paraffin wax; TAGA: Thermally annealed graphene aerogel; GNPs: Graphene nanoplatelets; PVDF: Poly (vinylidene fluoride); PDMS: Poly(dimethylsiloxane); MWCNTs: Multi-walled carbon nanotubes; MAPP: Ammonium polyphosphate wrapped MXene; CMC, Carboxymethyl cellulose, MG: Multilayer graphene.

References

1 Z. Peng, Q. Lv, J. Jing, H. Pei, Y. Chen and E. Ivanov, *Compos. Part B Eng.*, 2023, **251**, 110491.

2 X. Li, M. Sheng, S. Gong, H. Wu, X. Chen, X. Lu and J. Qu, *Chem. Eng. J.*, 2022, **430**, 132928.

3 M. Ma, X. Liang, W. Tao, Q. Peng, W. Shao, S. Chen, Y. Shi, H. He, Y. Zhu and X. Wang, *Compos. Struct.*, 2024, **342**, 118259.

4 W. Chu, J. Li, J. Lin, W. Li, J. Xin, F. Liu, X. He, Z. Ma and Q. Zhao, *Compos. Sci. Technol.*, 2024, **249**, 110489.

5 F. Ren, L. Ma, C. Li, T. Wu, J. Zhang, L. Pei, Y. Jin, Z. Sun, Z. Guo, P. Song and P. Ren, *Carbohydr. Polym.*, 2025, **356**, 123369.

6 T. Liu, H. Feng, L. Deng, C. Jin, H. Vahabi, M. R. Saeb and T. Kuang, *Nanoscale*, 2024, **16**, 21048–21060.

7 Y. Yang, R. Bi, W. Ren, Y. Sun, H. Zhao and H. Duan, *Compos. Sci. Technol.*, 2023, **243**, 110259.

8 G. Sang, P. Xu, C. Liu, P. Wang, X. Hu and Y. Ding, *Ind. Eng. Chem. Res.*, 2020, **59**, 15233–15241.

9 C. Liang, H. Qiu, Y. Han, H. Gu, P. Song, L. Wang, J. Kong, D. Cao and J. Gu, *J. Mater. Chem. C*, 2019, **7**, 2725–2733.

10 S. Zhang, J. Ye and X. Liu, *Colloids Surf. Physicochem. Eng. Asp.*, 2023, **656**, 130414.

11 X. Pei, G. Liu, H. Shi, R. Yu, S. Wang, S. Liu, C. Min, J. Song, R. Shao and Z. Xu, *Compos. Sci. Technol.*, 2023, **233**, 109909.

12 P. Zhang, H. Li, H. Liang, H. Wang, C. Yang, X. Shan, Q. Zhang and Y. Chen, *Mater. Today Commun.*, 2024, **38**, 108506.

13 Y. Zhang, S. Yang, Y. Liu, T. Gu and F. Liu, *J. Mater. Chem. A*, 2024, **12**, 27527–27539.

14 T.-B. Ma, H. Ma, K.-P. Ruan, X.-T. Shi, H. Qiu, S.-Y. Gao and J.-W. Gu, *Chin. J. Polym. Sci.*, 2022, **40**, 248–255.

15 Z. Zhang, G. Liu, J. Wu, X. Jiang, H. Liu and Z. Li, *Chem. Eng. J.*, 2025, **519**, 165710.

16 J. Lee and J. Kim, *Compos. Commun.*, 2021, **28**, 100935.

17 D.-L. Zhang, S.-N. Liu, H.-W. Cai, Q.-K. Feng, S.-L. Zhong, J.-W. Zha and Z.-M. Dang, *J. Materiomics*, 2020, **6**, 751–759.

18 X. Yang, S. Fan, Y. Li, Y. Guo, Y. Li, K. Ruan, S. Zhang, J. Zhang, J. Kong and J. Gu, *Compos. Part Appl. Sci. Manuf.*, 2020, **128**, 105670.

19 X. Chen, J. S. K. Lim, W. Yan, F. Guo, Y. N. Liang, H. Chen, A. Lambourne and X. Hu, *ACS Appl. Mater. Interfaces*, 2020, **12**, 16987–16996.

20 L. Wu, X. Liu, G. Wan, X. Peng, Z. He, S. Shi and G. Wang, *Chem. Eng. J.*, 2022, **448**, 137600.

21 W. Lee and J. Kim, *Polym. Test.*, 2021, **104**, 107402.

22 P. Jia, Y. Zhu, J. Lu, B. Wang, L. Song, B. Wang and Y. Hu, *Chem. Eng. J.*, 2022, **439**, 135673.

23 P. Zhang, X. Ding, Y. Wang, Y. Gong, K. Zheng, L. Chen, X. Tian and X. Zhang, *Compos. Part Appl. Sci. Manuf.*, 2019, **117**, 56–64.

24 Z. Tao, H. Zou, M. Li, S. Ren, J. Xu, J. Lin, M. Yang, Y. Feng and G. Wang, *J. Colloid Interface Sci.*, 2023, **629**, 632–643.

25 Z. Huang, C. Wang, L. Zhou and C. Wu, *Surf. Interfaces*, 2021, **26**, 101338.